A syntaxin 10–SNARE complex distinguishes two distinct transport routes from endosomes to the trans-Golgi in human cells

Ian G. Ganley, Eric Espinosa, and Suzanne R. Pfeffer

Department of Biochemistry, Stanford University School of Medicine, Stanford, CA 94305

Mannose 6-phosphate receptors (MPRs) are transported from endosomes to the Golgi after delivering lysosomal enzymes to the endocytic pathway. This process requires Rab9 guanosine triphosphatase (GTPase) and the putative tether GCC185. We show in human cells that a soluble NSF attachment protein receptor (SNARE) complex comprised of syntaxin 10 (STX10), STX16, Vti1a, and VAMP3 is required for this MPR transport but not for the STX6-dependent transport of TGN46 or cholera toxin from early endosomes to the Golgi. Depletion of STX10 leads to MPR missorting and hypersecretion of hexosaminidase. Mouse and rat cells lack STX10 and, thus, must use a different target membrane SNARE for this process. GCC185 binds directly to STX16 and is competed by Rab6. These data support a model in which the GCC185 tether helps Rab9-bearing transport vesicles deliver their cargo to the trans-Golgi and suggest that Rab GTPases can regulate SNARE–tether interactions. Importantly, our data provide a clear molecular distinction between the transport of MPRs and TGN46 to the trans-Golgi.

Introduction

Mannose 6-phosphate receptors (MPRs) carry newly synthesized lysosomal enzymes from the Golgi to early endosomes and then return to the TGN to retrieve additional cargo (Ghosh et al., 2003). However, MPRs cannot release their bound ligands upon arrival in early endosomes because they require a lower pH than typical endocytic receptors for efficient ligand release (Tong and Kornfeld, 1989). Thus, MPRs must pass through a compartment of pH ≤ 5.5 before returning to the Golgi to carry out their biological function.

In CHO cells, MPRs appear to traffic via so-called recycling endosomes before arrival in the Golgi, but these pH-neutral compartments also cannot support ligand release (Lin et al., 2004). Moreover, in many cell types, the majority of MPRs reside in more acidic late endosomes at steady state (Griffiths et al., 1988). The finding that the late endosomal Rab9 GTPase is required for MPR recycling (Lombardi et al., 1993; Riederer et al., 1994; Iversen et al., 2001; Ganley et al., 2004) supports a model in which MPRs travel through late endosomes before arrival at the TGN. Thus, MPRs may travel from early endosomes to recycling endosomes to late endosomes en route to the Golgi complex. We focus on this last stage in the MPR recycling process.

Rab9-dependent transport from late endosomes to the Golgi requires the Rab9 effectors p40 (Diaz et al., 1997) and TIP47 (Diaz and Pfeffer, 1998), a protein that recognizes the cytoplasmic domains of the two types of MPRs and packages them into nascent transport vesicles (Carroll et al., 2001). MPR recycling also utilizes a TGN-localized coiled-coil protein named GCC185 that is also a Rab9 effector (Reddy et al., 2006; Derby et al., 2007). GCC185 is a putative transport vesicle tether that contains a so-called GRIP domain at its C terminus (Luke et al., 2003).

SNARE proteins mediate the ultimate fusion of vesicles after they have docked at their corresponding target membrane (Jahn and Scheller, 2006). To date, the identity of the SNARE complex that mediates vesicle fusion in MPR recycling has remained unknown (Bonifacino and Rojas, 2006). A separate transport pathway carries certain proteins such as Shiga toxin, cholera toxin, and ricin from early endosomes to the Golgi complex (Spooner et al., 2006). This pathway utilizes a SNARE complex containing syntaxin 6 (STX6), STX16, Vti1a, and the v-SNAREs VAMP3 or VAMP4 as well as the Rab6A GTPase (Mallard et al., 2002) but not Rab9 GTPase (Iversen et al., 2001;

Correspondence to Suzanne R. Pfeffer: pfeffer@stanford.edu

Abbreviations used in this paper: CD, cation dependent; CI, cation independent; EEA1, early endosome antigen 1; MPR, mannose 6-phosphate receptor; STX, syntaxin.

The online version of this article contains supplemental material.

The Journal of Cell Biology, Vol. 180, No. 1, January 14, 2008 159–172
http://www.jcb.org/cgi/doi/10.1083/jcb.200707136

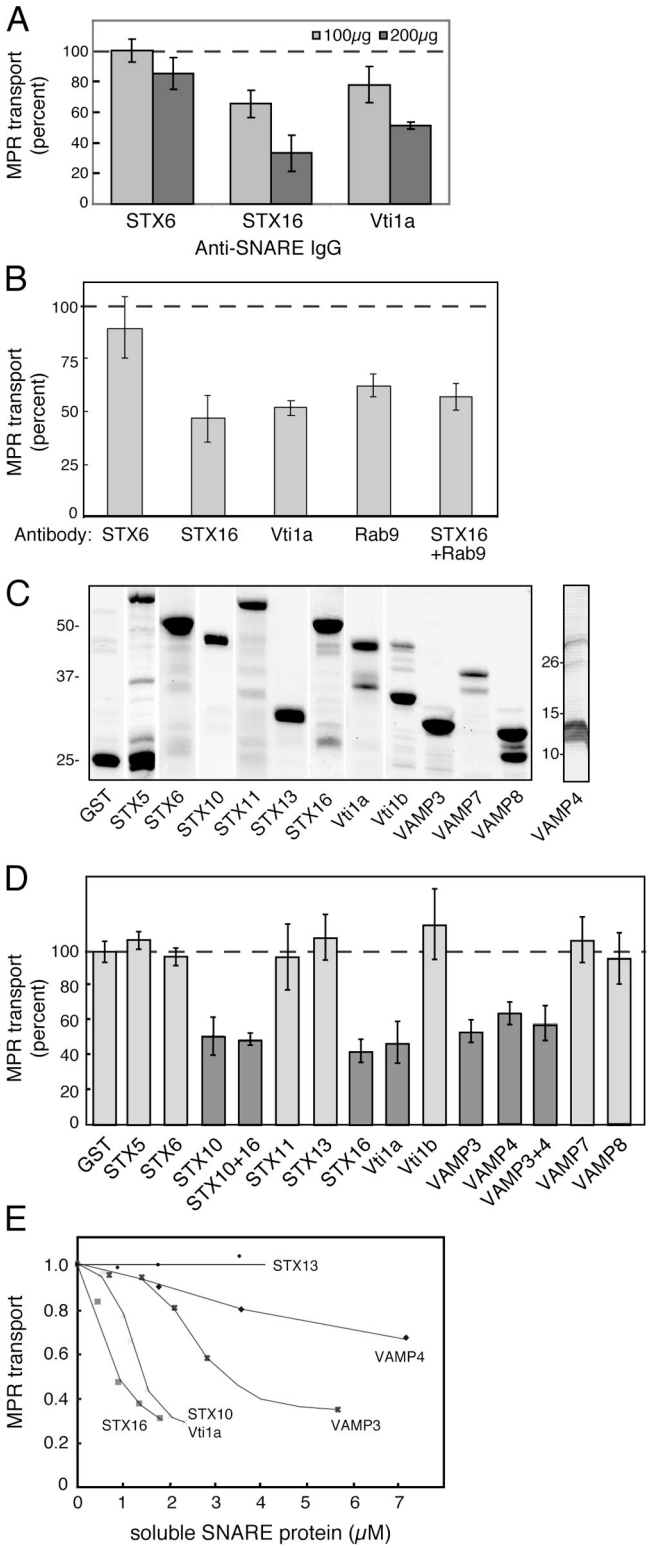

Figure 1. **Retrograde transport of MPRs to the TGN is mediated by STX10, STX16, Vti1a, and VAMP3.** (A) In vitro transport of CD-MPRs in reactions containing 100 μg/ml (light gray bars) or 200 μg/ml (dark GRAY bars) anti-SNARE IgG. Cytosol-dependent transport is expressed as a percentage of the control reaction containing the equivalent amount of nonspecific IgG. Error bars represent SD; data are from three independent experiments. (B) In vitro transport of MPRs in reactions containing 200 μg/ml of the indicated IgG. (C) Coomassie-stained SDS-PAGE of recombinant SNAREs used in D. Each lane contains 15 μg of purified protein except the lanes for STX10 and Vti1b, which contain 10 μg of purified protein. (D) In vitro transport of MPRs in reactions containing 100 μg/ml GST alone (3.8 μM), GST-tagged versions of soluble STX5 (1.8 μM), STX6 (1.9 μM), STX10 (2 μM), STX11 (1.8 μM), STX16 (1.9 μM), Vti1a (2.3 μM), Vti1b (2.3 μM), VAMP3 (2.8 μM), VAMP7 (2.7 μM), VAMP8 (2.6 μM), or thrombin-cleaved soluble domains of STX13 (3.5 μM) and VAMP4 (7.1 μM). (B and D) Error bars represent SD from at least two independent experiments performed in triplicate. The dashed line demarcates 100%. (E) In vitro transport of MPRs in reactions containing the indicated amounts of GST-soluble SNARE protein. Values are means from at least two independent experiments performed in triplicate.

Smith et al., 2006). A second SNARE complex comprised of STX5, GS28, Ykt6, and GS15 may also be involved in early endosome to Golgi transport (Tai et al., 2004), but this complex is most likely involved in retrograde transport through the Golgi. In addition, Lu et al. (2004) have shown a role for Golgin-97 in this process.

Recent work has shown that STX16 is needed for MPR recycling to the TGN (Saint-Pol et al., 2004; Amessou et al., 2007), which suggested that MPRs are transported together with Shiga toxin from early endosomes back to the Golgi and use the same STX6–STX16–Vti1a SNARE complex. In this study, we confirm a role for STX16 but show that this t-SNARE acts as part of a distinct STX10-containing SNARE complex to mediate MPR recycling to the TGN. Although TGN46 and cholera toxin require STX6, MPR recycling does not: the STX10-containing SNARE complex functions specifically for MPR recycling in human cells. One component of the STX10 complex binds to the putative tether GCC185 directly, and this interaction is competed by the Rab6 GTPase. This study identifies key molecular components that distinguish two membrane transport pathways to the Golgi.

Results

Two approaches were taken to identify the SNARE proteins responsible for MPR transport to the Golgi. First, we tested the ability of antibodies to block the transport of cation-dependent (CD) MPR to the TGN in vitro. SNARE identification was initially hindered by the lack of cross-reactivity of anti-SNARE antibodies with the CHO cell components of our original in vitro transport assays (Itin et al., 1997). To circumvent this, we re-established our in vitro transport assay using an HEK293 human cell line that stably expresses a tagged version of the CD-MPR containing an N-terminal His tag for purification, a myc-tag for localization, and a consensus tyrosine sulfation site that can be modified by tyrosine sulfotransferase upon its arrival at the TGN (Itin et al., 1997).

As shown in Fig. 1 A, anti-STX16 and -Vti1a antibodies inhibited in vitro transport in a concentration-dependent manner, but anti-STX6 antibodies did not. STX6 is required for the transport of Shiga toxin and cholera toxin from early endosomes to the Golgi complex (Mallard et al., 2002). Three monoclonal and one polyclonal anti-Rab6 antibody were tried without effect (Fig. S1 A, available at http://www.jcb.org/cgi/content/full/jcb.200707136/DC1). This observation provided an important molecular distinction between these two transport pathways, which have already been shown to differ in their requirements

for the Rab9 GTPase (Iversen et al., 2001) and the putative tether, Golgin-97 (Lu et al., 2004; Reddy et al., 2006).

To determine whether these SNARE antibodies inhibited a Rab9-dependent step, we tested whether the addition of both anti-Rab9 IgG and anti-STX16 IgG led to an even greater level of inhibition. As shown in Fig. 1 B, anti-STX16 and anti-Rab9 antibodies each inhibited in vitro transport ~40–50%. When added together, no further inhibition was observed. This suggests that Rab9 and STX16 antibodies are inhibiting the same transport process in vitro.

As a second independent test for SNARE involvement, we expressed and purified soluble forms of 12 TGN and endosome-localized SNARE proteins (Fig. 1 C) and tested their ability to inhibit in vitro transport reactions by presumably forming nonfunctional complexes with endogenous SNARE proteins. In agreement with the antibody inhibition data (Fig. 1 A), soluble GST-tagged STX16 and Vti1a proteins inhibited transport ~50–60% (Fig. 1 D). Removal of GST by thrombin cleavage of GST-STX16 yielded the same level of transport inhibition (41 ± 0.1% MPR transport relative to control reactions). In addition, STX10 and soluble VAMP3 and 4 inhibited transport (Fig. 1 D). In contrast, soluble STX5, 6, 11, 13, Vti1b, and VAMP7 and 8 were without significant effect (Fig. 1 D).

STX6 and 13 function in early endosome fusion (McBride et al., 1999; Mills et al., 2001; Sun et al., 2003; Brandhorst et al., 2006); VAMP7 and 8 are involved in early to late endosome fusion (Antonin et al., 2000a,b; Pryor et al., 2004). The inability of these soluble SNAREs to inhibit in vitro transport confirms that we are indeed inhibiting the late endosome to TGN transport of MPRs and not an interendosomal transport process.

Analysis of the concentration dependence of the inhibition observed showed that transport could be inhibited as much as 70% with ~2 μM STX10, STX16, and Vti1a (Fig. 1 E). VAMP3 and 4 were less potent but also showed concentration-dependent inhibition. When evaluated on a concentration basis (Fig. 1 E), VAMP3 was significantly more potent than VAMP4 and is likely to be the more relevant vesicle SNARE for this reaction. The control SNARE protein STX13 failed to inhibit transport when added to similar concentrations. Together, these experiments implicate a SNARE complex comprised of STX10, STX16, Vti1a, and VAMP3 in the transport of MPRs from late endosomes to the Golgi complex. This set of SNAREs includes one member each from the categories Qa, Qb, Qc, and R SNAREs that are required to form a functional SNARE complex (Jahn and Scheller, 2006). Further evidence suggesting that these SNAREs function in a common step (and thus are members of the same complex) is shown in Fig. 1 D; the inhibitory effects of STX10 and 16 were not additive. This specific SNARE complex (STX10–STX16–Vti1a–VAMP3) has been detected in living cells (Wang et al., 2005), but its precise function was unknown until now.

To verify the physiological significance of our in vitro experiments, we tested the consequences of soluble SNARE protein overexpression in cultured cells. A block in MPR recycling caused by an inhibitory SNARE protein should decrease the level of MPRs available within the Golgi to transport newly synthesized lysosomal hydrolases efficiently. Under these conditions, hydrolases would be missorted and secreted. Thus, hexosaminidase secretion can be used to monitor a block in MPR trafficking. We have shown this to be true in cells expressing a dominant inhibitory Rab9 protein (Riederer et al., 1994) or depleted of the putative tether, GCC185 (Reddy et al., 2006).

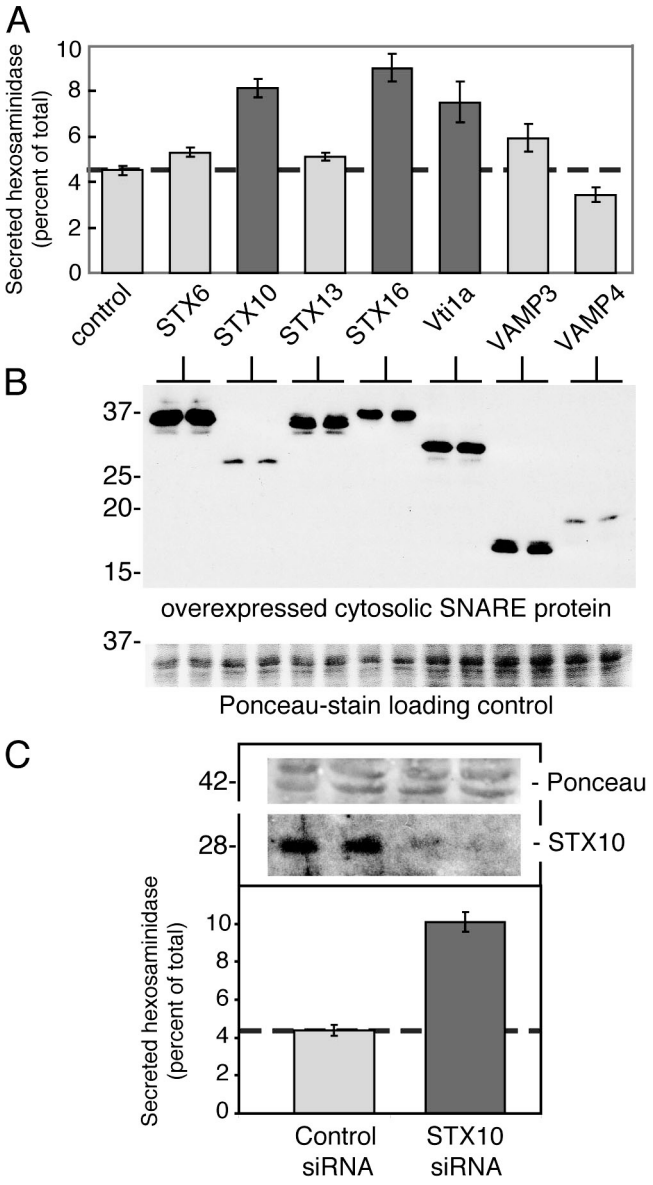

Figure 2. **Hexosaminidase secretion is increased in cells when STX10, STX16, or Vti1a function is compromised.** (A) HeLa cells grown in 6-cm dishes were either mock transfected (control) or transfected with the indicated myc-tagged cytosolic SNARE and incubated in fresh media for 8 h to collect secreted hexosaminidase. (B) Immunoblot of overexpressed SNARE proteins from the cells analyzed in A and a portion of the Ponceau S–stained filter as a loading reference. Proteins were detected with anti-myc tag antibody. (C) Hexosaminidase secretion from control or STX10-depleted HeLa cells. The top panel shows a Ponceau S–stained immunoblot membrane (top bar) of HeLa cell lysate reacted with antibodies to monitor STX10 depletion. Numbers at the right in B and C indicate M_r in kilodaltons. (A and C) Values are means from at least three independent experiments performed in triplicate; error bars represent SD.

Expression of soluble versions of STX10, STX16, and Vti1a but not STX6, STX13, or VAMP4 led to roughly a doubling in the amount of hexosaminidase secreted (Fig. 2 A). Comparison of the levels of exogenous SNARE protein expression (Fig. 2 B)

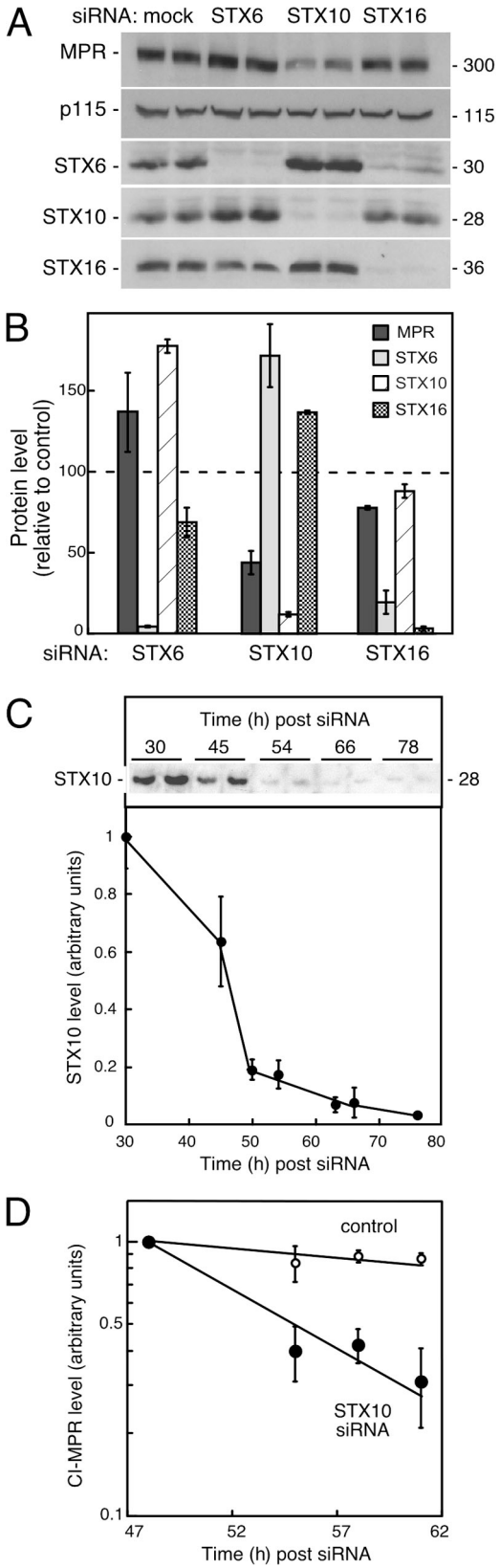

Figure 3. **MPRs are destabilized in cells depleted of STX10.** CI-MPR and SNARE protein levels in HEK293 cells transfected with the indicated siRNAs. (A) Immunoblot. (B) Quantitation of the data shown in A. Values are from two independent experiments, normalized to p115 levels relative to protein levels in control transfected cells. Error bars represent SD. (C) Kinetics of STX10 depletion after siRNA transfection of HEK293 cells. The inset shows an immunoblot of STX10 monitored at the indicated times. Quantitation of those data is graphed; two independent experiments performed in duplicate are presented. (D) Half-life of CI-MPRs in cells depleted of STX10 measured at the times indicated after siRNA transfection. Numbers at the right in A and C indicate M_r in kilodaltons.

shows that STX10 was the most potent inhibitor. VAMP4 was poorly expressed; therefore, the results for this SNARE are inconclusive. Only a slight increase in hexosaminidase secretion was seen in cells overexpressing VAMP3. Together, these data support the in vitro findings (Fig. 1) and the conclusion that a STX10–STX16–Vti1a-containing complex is needed for MPR recycling in living cells. In addition, soluble v-SNAREs were less potent inhibitors than soluble t-SNAREs both in vitro (Fig. 1) and upon expression in cultured cells (Fig. 2).

We confirmed the importance of the STX10 t-SNARE in MPR trafficking by siRNA depletion (Fig. 2 C, inset). In cells depleted of ~90% of their STX10 content, hexosaminidase secretion was stimulated ~2.5-fold (Fig. 2 C). Thus, by two independent criteria, STX10 is required for proper lysosomal enzyme sorting in living cells.

Loss of STX10 enhances MPR degradation

Steady-state levels of MPRs were also significantly decreased in cells depleted of STX10 and, to a lesser extent, in cells depleted of STX16 (Fig. 3 A) relative to a control protein, p115. This is reminiscent of the increased turnover of MPRs observed when cells are depleted of TIP47, Rab9, or GCC185 (Diaz and Pfeffer, 1998; Ganley et al., 2004; Reddy et al., 2006) or seen upon the loss of Retromer and PIKfyve proteins (Arighi et al., 2004; Seaman, 2004; Rutherford et al., 2006).

Interestingly, siRNA depletion of STX16 led to a concomitant 80% loss of STX6 with little change in STX10; the depletion of STX6 led to a 30% loss of STX16. This suggests that the majority of STX6 is complexed to a significant fraction of STX16 in the cell and that STX16 is an important stabilizer of STX6. Cells depleted of STX10 showed increased levels of STX6 (60%) and STX16 (40%; Fig. 3, A and B). In contrast, the depletion of STX6 led to a 60% increase in STX10 levels. It is possible that the depletion of one SNARE frees up STX16 to provide additional stabilization for another partner SNARE protein.

The loss of MPRs in STX10-depleted cells was caused by an increase in their degradation rate as measured in a pulse-chase labeling experiment. Cells were transfected with STX10 siRNA at time zero, and the loss of STX10 protein was monitored. At 45 h of siRNA treatment, STX10 protein was decreased by 36%; by 54 h, it was decreased by 83% (Fig. 3 C). Cells were pulse labeled with [^{35}S]methionine and cysteine, and the chase was begun at a time when STX10 began to be significantly depleted. MPR levels were then determined at various times by immunoprecipitation. As shown in Fig. 3 D, cells depleted of STX10 showed significantly increased MPR degradation compared with control-treated cells. The half-life of MPRs was estimated to be ~13 h in the absence of STX10, which was much shorter than that of control cells (>36 h) under these conditions. This confirms the importance of STX10 for MPR stability and, by inference, MPR trafficking.

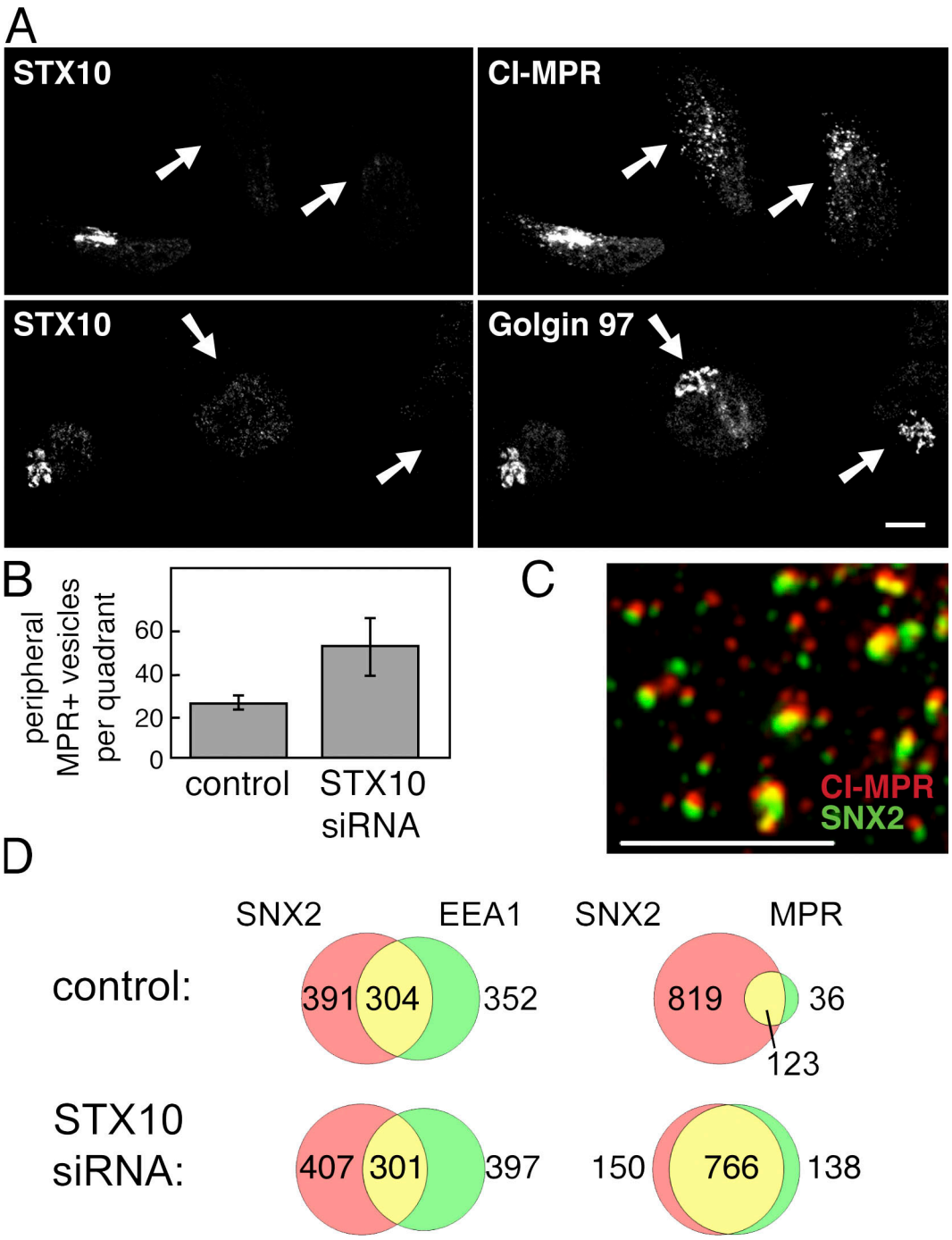

Figure 4. **Depletion of STX10 leads to CI-MPR dispersal to sorting nexin-2–positive structures but does not disrupt Golgin 97 localization.** (A) Summation of confocal z sections of HeLa cells treated with STX10 siRNA and double labeled with rabbit anti-STX10 and mouse anti–CI-MPR (top) or rabbit anti-STX10 and mouse anti–Golgin 97 (bottom). Arrows point to cells depleted of STX10. Bar, 10 μm. (B) Quantitation of CI-MPR dispersal in cells depleted of STX10. Peripheral CI-MPR–positive vesicles were determined as described in Materials and methods. The mean number of vesicles from three separate cells normalized for cell area is shown. Error bars represent SD. (C) Deconvolution microscope image showing colocalization of endogenous CI-MPR (stained red with mouse antibody) and sorting nexin-2 (stained green with rabbit antibody) in the periphery of a HeLa cell depleted of STX10. Bar, 5 μm. (D) Venn diagrams representing the quantitation of colocalization between sorting nexin-2 and EEA1 or sorting nexin-2 and CI-MPR in nonperinuclear regions of control and STX10-depleted HeLa cells. Vesicles were from nine (control) or seven (STX10 depleted) separate cells from two independent experiments. Venn diagrams are correctly scaled for percentage overlap to permit the direct comparison of antigens in each vesicle population.

MPR missorting in cells lacking STX10

The missorting of MPRs in cells depleted of STX10 was confirmed by light microscopy. As shown in Fig. 4 A, cells containing STX10 showed a typical perinuclear concentration of cation-independent (CI) MPRs (Fig. 4 A, top; cell at bottom left). In contrast, cells depleted of STX10 (Fig. 4 A, arrows) showed highly dispersed staining for CI-MPRs (Fig. 4 A, top right; arrows). Under these conditions, the TGN was intact as determined by the

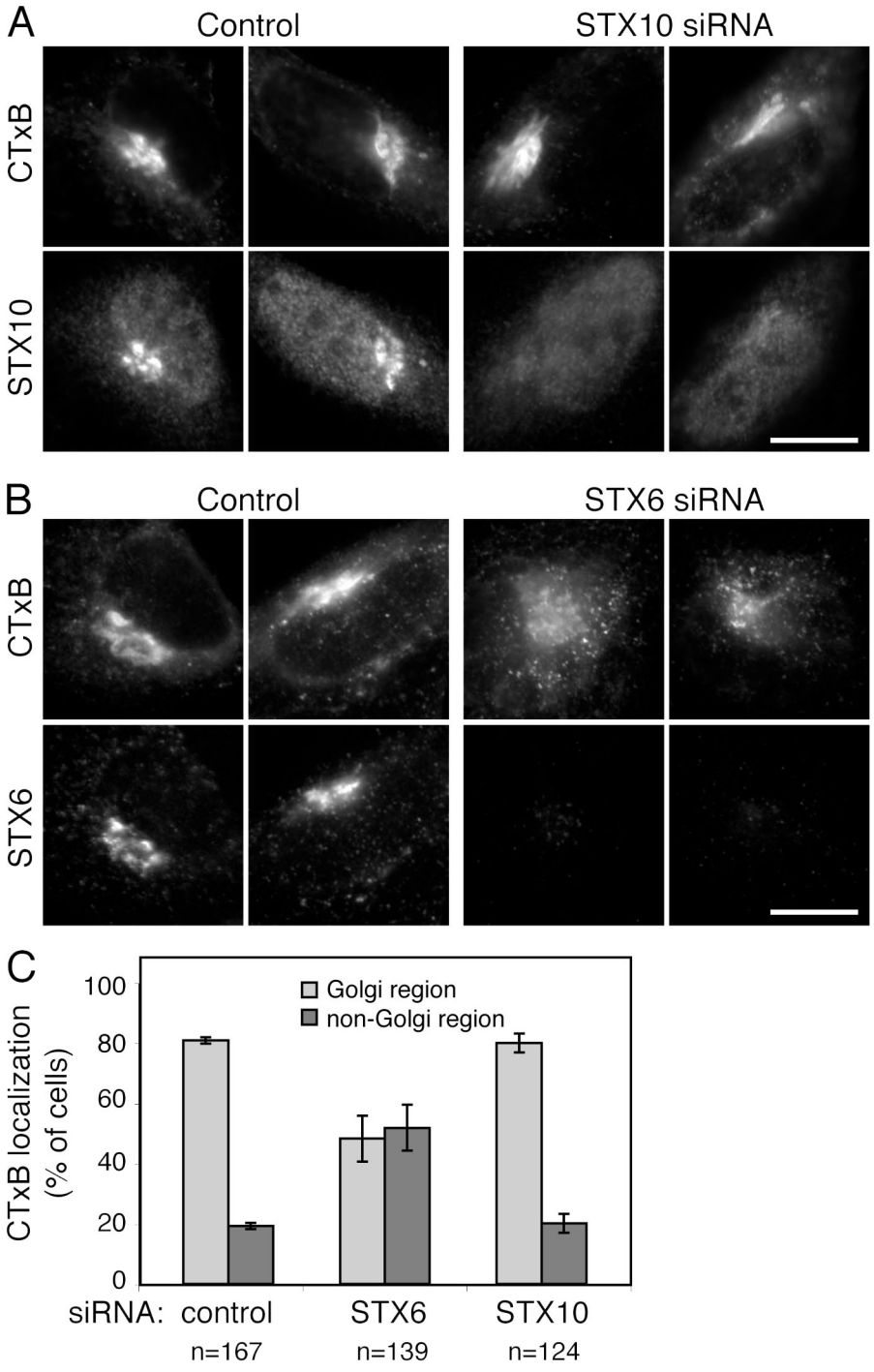

Figure 5. **Cholera toxin B fragment transport in cells depleted of STX10 or 6.** (A) HeLa cells were treated with control siRNA (left) or STX10 siRNA (right) and were allowed to internalize AlexaFluor488-conjugated cholera toxin B (CTxB) for 30 min followed by a 30-min chase. Cholera toxin B or rabbit anti-STX10 staining (detected with AlexaFluor 94 anti–rabbit) is indicated at the left. (B) Control (left) and STX6-depleted (right) HeLa cells were treated with cholera toxin B as in A. Cholera toxin B and mouse anti-STX6 staining (detected with AlexaFluor594 anti–mouse) of the same cells is indicated at the left. (C) Quantitation of the data shown in A and B. The numbers of cells counted (*n*) were from three independent experiments, and error bars represent SD. Bars, 10 μm.

localization of the TGN protein Golgin-97 (Fig. 4 A, bottom). Therefore, in cells lacking STX10, CI-MPRs are mislocalized to vesicles that are dispersed throughout the cytoplasm. Quantitation of the peripheral vesicles showed that their number increased more than twofold in cells depleted of STX10 (Fig. 4 B).

Characterization of the accumulated vesicles revealed that they contain sorting nexin-1 (not depicted) and sorting nexin-2 proteins (Fig. 4 C), which are constituents of the retromer complex that is important for MPR recycling to the trans-Golgi complex (Arighi et al., 2004; Seaman, 2004; Rojas et al., 2007). Indeed, 85% (766/904) of peripheral MPR-positive vesicles were sorting nexin-2 positive in STX10-depleted cells (Fig. 4, C and D). A significant proportion of sorting nexin-2 protein colocalizes with early endosome markers such as early endosome antigen 1 (EEA1; Arighi et al., 2004; Seaman, 2004; Carlton et al., 2005; Rojas et al., 2007). In the current study, EEA1 was present on 44% (304/695) of sorting nexin-2–positive structures in control cells; only 123/942 (13%) of the peripheral sorting nexin-2 structures contained CI-MPRs, and few peripheral MPR structures were observed (159; Fig. 4 D). Upon STX10 depletion, 43% (301/708) of sorting nexin-2–positive vesicles contained EEA1, and 84% (766/916) contained CI-MPRs. As before, we saw

a significant increase in peripheral MPR-positive structures (904/159). These peripheral MPRs showed a similar degree of overlap with EEA1 as sorting nexin-2 in STX10-depleted cells (~45%; unpublished data). In summary, upon the loss of STX10, the newly peripheral MPRs are tightly associated with sorting nexin-2 in small peripheral structures; at least some of these represent early endosomes because of their content of EEA1.

Are the peripheral MPR-containing structures that accumulate in STX10-depleted cells transport vesicle intermediates? If so, they would be expected to contain Rab9, which resides on the surface of vesicles traversing from late endosomes to the trans-Golgi (Barbero et al., 2002). HeLa cells depleted of the putative tether GCC185 also accumulate MPRs in peripheral vesicles, the majority of which contain Rab9 protein (Reddy et al., 2006). In contrast, in STX10-depleted cells, only 18% (15/84) of MPR-containing, peripheral vesicles also contained Rab9 (unpublished data). This suggests that MPRs are blocked in a prelate endosome compartment before a Rab9-dependent vesicle transfer process. Wang et al. (2005) showed that cells depleted of STX10 display an alteration in transferrin receptor localization. If STX10 participates in more than one transport event, its depletion could lead to the accumulation of MPRs in a peripheral Rab9-negative prelate endosome compartment. Importantly, because our in vitro transport assay measures transport from a late endosome compartment (Goda and Pfeffer, 1988), we are able to discern a specific role for STX10 in transport from that compartment to the Golgi complex.

STX10 functions in the late endosome to Golgi pathway

To verify that STX10 is required at the TGN for the receipt of late endosome but not early endosome-derived cargoes, we tested whether cells depleted of this t-SNARE were competent to transport cholera toxin B from early endosomes to the Golgi complex. For these experiments, fluorescent cholera toxin B fragment was internalized by receptor-mediated endocytosis for 30 min, and its arrival to the TGN was monitored microscopically after an additional 30 min. As shown in Fig. 5 A, the depletion of STX10 did not compromise the ability of HeLa cells to transport fluorescent cholera toxin B fragment from the early endocytic pathway to the TGN. In contrast, consistent with previous papers studying Shiga toxin (Mallard et al., 2002; Wang et al., 2005), the disruption of STX6 blocked this transport step (Fig. 5 B). As was true for STX10 depletion, the loss of STX6 did not alter the TGN, as monitored by immunostaining for Golgin-97 (not depicted) or GCC185 (Fig. 6), suggesting that cholera toxin mislocalization in STX6-depleted cells is not simply caused by Golgi complex disruption. Quantitation of these experiments revealed a block in cholera toxin transport in >50% of cells analyzed (Fig. 5 C). This morphological determination provides a minimum estimate of the extent of a block in transport, as only severely impaired cells are scored.

As an independent test of the specificity of STX10, we also examined the localization of TGN46, a protein that shuttles between endosomes and the Golgi complex (Fig. 6). Cells depleted of STX10 showed perfect Golgi localization of TGN46 (Fig. 6, top; arrows). In contrast, cells depleted of STX6 showed

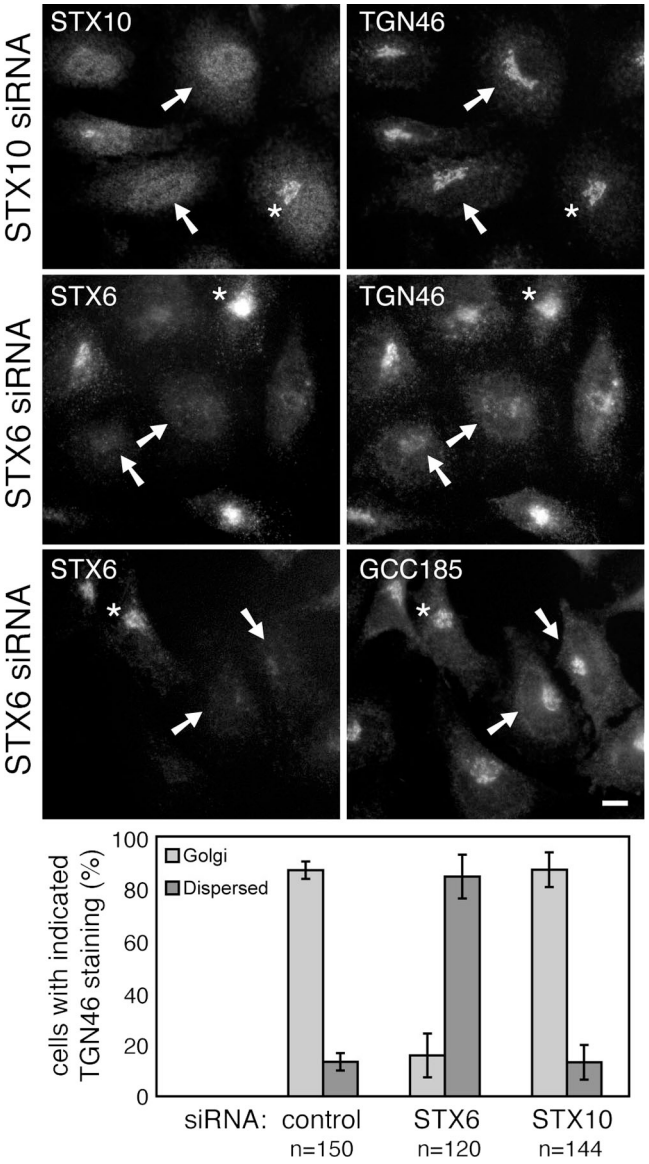

Figure 6. **TGN46 transport in cells depleted of STX10 or S6.** HeLa cells were treated with STX10 siRNA (top) or STX6 siRNA (middle) and were stained for the indicated proteins; TGN46 was detected with sheep antibody and AlexaFluor594 anti–sheep antibodies. Arrows point to SNARE-depleted cells, and asterisks mark undepleted cells. The bottom panel presents quantitation of the data shown. The numbers of cells counted (*n*) were from two independent experiments; error bars represent SD. Bar, 10 μm.

a vesicular pattern for TGN46 in >80% of cells scored (Fig. 6, middle; arrows). This was not caused by disruption of the TGN, at least by the criteria of GCC185 staining (Fig. 6, bottom; arrows).

These data directly show that the transport of proteins from early and late endosomes to the Golgi complex are mediated by distinct SNARE protein complexes: a SNARE complex containing STX6, STX16, and Vti1a mediates the receipt of cargo from early endosomes, whereas a complex containing STX10, STX16, and Vti1a mediates the receipt of cargo from late endosomes. Moreover, they reveal that the steady-state localization of TGN46 is sensitive to the loss of STX6, a finding that suggests that this protein follows a transport route that is shared with cholera toxin but is distinct from MPRs.

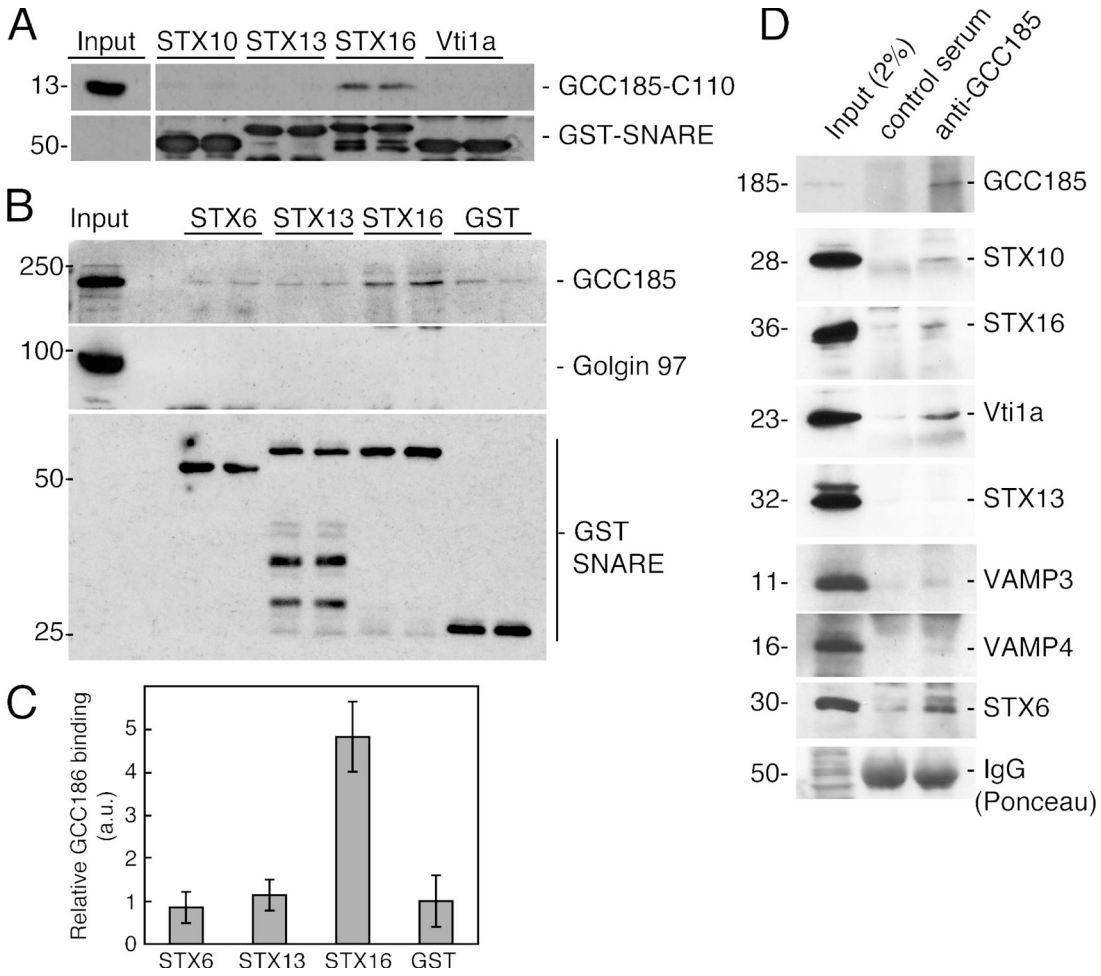

Figure 7. **STX16 interacts directly and specifically with GCC185.** (A) GST-tagged cytosolic SNAREs were incubated with purified GCC185–C-110. Tagged SNAREs were recovered by glutathione–Sepharose beads, and the bound proteins were analyzed by SDS-PAGE and immunoblotting with rabbit anti-GCC185 (top) to detect bound C-110 or with rabbit anti-GST (bottom) to detect input SNAREs. Input lane at the left (top row) represents 2% of the total GCC185–C-110 used in each reaction. (B) STX16 interacts with full-length GCC185. Recombinant GST-tagged soluble SNARE proteins were incubated with K562 cell cytosol; the tagged SNAREs were then retrieved with glutathione–Sepharose beads. Bound proteins were analyzed by SDS-PAGE and immunoblotting to detect bound, full-length GCC185 (top), full-length Golgin97 (middle), or resin-bound GST-SNARE proteins (bottom). The input lane represents 1% of the total cytosol used in each reaction. (C) Quantitation of the data shown in B. Error bars represent SD from two independent experiments. (D) STX10, STX16, and Vti1a coimmunoprecipitate with GCC185. HeLa cells expressing the myc-tagged soluble SNAREs were lysed and incubated with equal amounts of either control serum or anti-GCC185 serum. Immune complexes were isolated with protein A–agarose, and bound proteins were analyzed by SDS-PAGE and immunoblotting with either rabbit anti-GCC185 serum (top) or mouse anti-myc antibody to detect exogenous SNARE proteins. A Ponceau S–stained region of the gel is shown as a loading control for IgG at the bottom. Numbers next to the gels in A, B, and D indicate M_r in kilodaltons.

A STX10 SNARE complex component binds the GCC185 tether

Essentially every putative tether studied to date interacts with cognate SNARE proteins (for review see Lupashin and Sztul, 2005). Thus, we were interested to test whether components of the STX10 complex interact with GCC185. GCC185 is a long coiled-coil protein that is required for MPR transport to the Golgi complex in vitro and in vivo (Reddy et al., 2006). In addition, GCC185 binds directly to the Rab9 GTPase, which is also needed for this transport process (Reddy et al., 2006).

We incubated purified, soluble SNARE proteins with recombinant GCC185 protein and analyzed bound proteins by immunoblotting. For these experiments, a GCC185 fragment comprised of the 110 C-terminal–most amino acids (C-110) was used. Importantly, the GCC185 C terminus bound directly to GST-STX16 but not to GST-STX10, -STX13, or Vti1a (Fig. 7 A). These data demonstrate that STX16 has the capacity to bind directly to GCC185. Although the binding is of low efficiency, it is specific.

We next tested whether full-length cytosolic GCC185 bound to immobilized SNARE proteins. In this case, GST-tagged STXs were incubated with cytosol; bound proteins were collected on glutathione–Sepharose beads and analyzed by immunoblotting. As shown in Fig. 7 B (top), full-length GCC185 bound to immobilized STX16 but did not show significant interaction with STX6, STX13, or the GST control (Fig. 7 C). In contrast, the structurally related Golgin-97 failed to bind to any of these SNARE proteins (Fig. 7 B, middle). This was somewhat surprising, as Golgin-97 is implicated in early endosome to TGN transport (Lu et al., 2004), and it might have shown binding to STX6 or 16, which participate in that transport step. In summary, these data confirm the ability of STX16 to bind specifically to full-length GCC185.

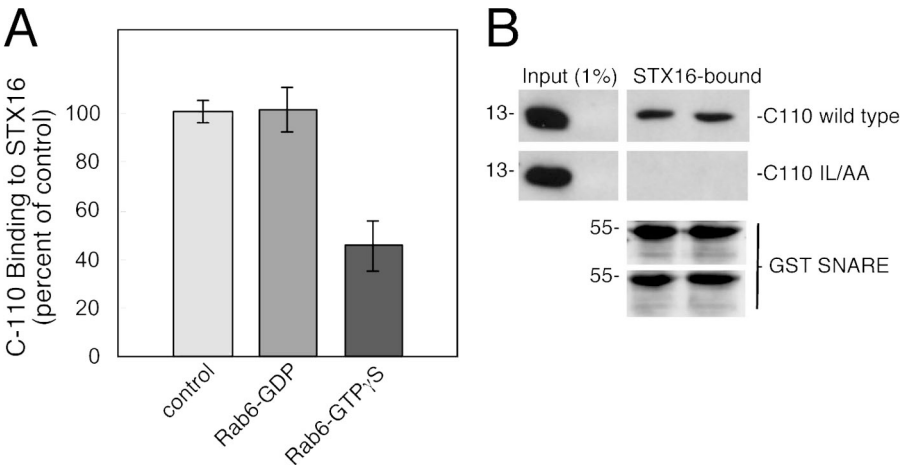

Figure 8. **Rab6 competes with STX16 for GCC185 binding.** (A) Purified, GCC185–C-110 and GST-soluble STX16 were incubated together, either alone or with Rab6 preloaded with GDP or GTPγS. GST-STX16 was recovered with glutathione–Sepharose beads; the bound GCC185–C-110 was analyzed by SDS-PAGE, and the immunoblot was probed with anti-GCC185 antibody. Immunoblots were quantified; the amount of GCC185–C-110 binding to STX16 relative to binding in the absence of Rab protein (control) from two independent experiments is shown. Error bars represent SD. (B) Equal amounts of purified GCC185–C-110 wild type or GCC185–C-110 IL/AA were incubated with GST-tagged soluble STX16. GST-STX16 was recovered with glutathione–Sepharose beads, and the bound proteins were analyzed by SDS-PAGE and immunoblotting with rabbit anti-GCC185 (top) to detect C-110 or with rabbit anti-GST (bottom) to detect STX16. Numbers at the left indicate M_r in kilodaltons.

STX16 could interact with GCC185 alone or as part of an intact SNARE complex. As shown in Fig. 7 D, incubation of cell extracts with anti-GCC185 antiserum led to the coimmunoprecipitation of small amounts of coexpressed, myc-tagged, soluble STX10, STX16, and Vti1a but not STX13, VAMP3, or VAMP4. This protocol would yield an underestimate of protein interactions because the initial GCC185 immunoprecipitation was of low efficiency (Fig. 7 D, top). Together, these data suggest that GST-STX10 and Vti1a can interact with GCC185 indirectly as part of an STX16-containing complex of t-SNARE proteins (Fig. 7 A).

If this conclusion is correct, STX16 might also mediate the interaction of GCC185 with the STX6–STX16–Vti1a complex. As shown at the bottom of Fig. 7 D, myc-tagged soluble STX6 was also coimmunoprecipitated with GCC185 antibodies. Again, this interaction was indirect, as full-length GCC185 failed to bind to immobilized STX6 protein (Fig. 7 B). However, we found no evidence that GCC185 interacts functionally with this complex in vivo, as the depletion of GCC185 did not prevent cholera toxin transport to the Golgi (Fig. S1 B). It should be noted that Derby et al. (2007) reported a requirement for GCC185 in Shiga toxin transport, but the Golgi complex was much more disrupted in those siRNA depletion experiments than seen in our studies, and Golgin-97 may have been codepleted upon the efficient loss of GCC185 (Reddy et al., 2006).

The ability of STX16 to bind to the GCC185 C terminus led us to test whether Rab GTPase binding might compete for this interaction because we have shown that the GCC185 C terminus also contains a Rab-binding site (Reddy et al., 2006). The C-110 fragment binds to both Rab6 and Rab9 GTPases but not Rab1 or Rab5 GTPases (Reddy et al., 2006; Schweizer Burguete et al., 2008), and Rab binding might regulate SNARE interaction. As shown in Fig. 8 A, STX16 binding to GCC185 was decreased when reactions contained Rab6-GTP. At the same concentrations, Rab9 had less of an effect (unpublished data). Competition was specific for the active Rab protein in that Rab6-GDP failed to compete with STX16 for GCC185 binding. A mutant GCC185 protein construct (I1588A/L1595A) that fails to bind Rab GTPases (Schweizer Burguete et al., 2008) also failed to bind STX16 (Fig. 8 B), which is consistent with these proteins sharing interaction sites on GCC185. Failure to bind was not the result of protein misfolding, as the mutant protein is entirely dimeric and soluble (unpublished data).

In summary, these data demonstrate a role for STX10–STX16–Vti1a and VAMP3 in the transport of MPRs (but not TGN46 or cholera toxin) from late endosomes to the TGN. In addition, the putative tether for this transport reaction, GCC185, binds to the t-SNARE complex that mediates vesicle fusion. Finally, the ability of a Rab GTPase that would be present at the target membrane to regulate SNARE–tether interactions implies that Rabs may regulate such interactions during or after vesicle docking and fusion.

Discussion

We have shown here that the t-SNAREs STX10, STX16, and Vti1a and the v-SNARE VAMP3 participate in the recycling of MPRs from late endosomes to the Golgi complex. Antibodies specific for several of these proteins interfered with transport of the CD-MPR in vitro. In addition, overexpression of most of these proteins in cultured cells triggered lysosomal enzyme missorting, as detected by hypersecretion of the lysosomal enzyme hexosaminidase. This assay monitors the functions of both CI- and CD-MPRs. CI-MPRs were also destabilized in STX10-depleted cells, further supporting a requirement for this t-SNARE in MPR trafficking in vivo. Moreover, as would be expected for an MPR-recycling t-SNARE, the depletion of STX10 from cells led to the dispersal of endogenous CI-MPRs to peripheral vesicles. These vesicles were decorated with the retromer subunits sorting nexin-1 and -2, which are also important for MPR recycling to the Golgi (Arighi et al., 2004; Seaman, 2004; Rojas et al., 2007). These findings place the retromer complex upstream of both STX10 function and the GCC185 tethering complex in MPR transport. Together, our data suggest that STX10, STX16, Vti1a, and VAMP3 are important for the trafficking of both CD- and CI-MPRs. To our

knowledge, this is the first study to assign a role to STX10 in a specific transport step, that of fusion of MPR-containing vesicles at the TGN. In addition, we present evidence that is consistent with a possible additional role for STX10 in the fusion of retromer-positive structures with a later endosomal compartment. However, it is important to note that the STX10 gene is absent from rats and mice, which implies that another mechanism must replace STX10 function in these organisms. There are numerous examples of molecular differences in fundamental processes between humans and mice and rats. Receptors used by natural killer cells are of entirely different structural classes (Parham, 2005). The G protein–coupled thrombin receptors in humans and mice are distinct and activated by rather different mechanisms (Coughlin, 2005). In membrane traffic, most vertebrates except rats and mice express the CHC22 clathrin isoform that is encoded on human chromosome 22 (Wakeham et al., 2005). The precise role of CHC22 will be interesting and important to determine even if it is not present in rats and mice.

A search of the Ensembl genome database (Hubbard et al., 2007) reveals that in addition to humans, 11 diverse organisms contain an STX10 homologue in addition to STX6. These include chimpanzees, cows, dogs, a rodent (*Spermophilus tridecemlineatus*), fugu fish, and frogs, and the list is likely to increase when more genomes become available. Expression data from expressed sequence tag, sage, and microarray experiments (Skrabanek and Campagne, 2001; Huminiecki et al., 2003) show that STX10 has a ubiquitous expression profile that is essentially identical to that of STX6. However, STX10 and 6 are only 61% identical (75% similar) in sequence, and our data show that the proteins have very distinct functions in vitro and in vivo. Future experiments will reveal the solution used by rats and mice to transport MPRs to the Golgi.

A recent study by Wang et al. (2005) suggested that STX10 may not be essential for MPR recycling. However, these conclusions were based on a modest morphological change in MPR localization. In this study, different STX10 siRNA target sequences were used, resulting in a more efficient depletion of STX10 and a significant change in MPR localization. In addition, in vitro biochemical approaches as well as in vivo lysosomal hydrolase sorting assays (in response to protein depletion or overexpression) confirm a role for STX10 in MPR recycling.

Recent work has suggested that an STX5-containing SNARE complex may also be involved in endosome to Golgi recycling of MPRs (Amessou et al., 2007). However, siRNA depletion of STX5 led to a loss in Golgi integrity, making it difficult to rule out nonspecific effects caused by disruption of the target membrane. In addition, that study used a chimera of GFP tagged to the transmembrane and cytosolic domains of CI-MPR, and this type of construct has been shown to traffic differently than wild-type MPRs (Waguri et al., 2006). The experiments presented here show a clear, unambiguous role for the STX10-containing SNARE complex in MPR recycling by several independent criteria. Importantly, soluble STX5 t-SNARE was without effect in our in vitro transport assay (Fig. 1).

To date, we have demonstrated that depletion of Rab9 GTPase, the TIP47 cargo selection protein, the GCC185 putative tether, and STX10 all interfere with MPR trafficking in vitro and in vivo. Upon the depletion of components thought to mediate transport vesicle formation (Rab9 and TIP47), MPRs are destabilized and subject to premature degradation as a result of missorting to the lysosome. Loss of components believed to be important for vesicle docking and fusion leads to the accumulation of MPRs in small peripheral vesicles. In the case of GCC185, these vesicles carry Rab9 and do not represent early endosomes because they do not contain Rab5 or EEA1 (Aivazian et al., 2006; Reddy et al., 2006). Thus, these vesicles may represent transport intermediates. In STX10-depleted cells, the peripheral vesicles are distinct from those that accumulate in the absence of GCC185 and are likely to represent a block at a prelate endosome stage because they do not contain Rab9 GTPase. STX10 binds STX13 (Wang et al., 2005), which does not participate in late endosome to TGN transport but has been implicated in transferrin receptor recycling (Prekeris et al., 1998). Also, multiple roles for a t-SNARE are not uncommon: for example, STX6 is needed for homotypic fusion of early endosomes and immature secretory granules, exocytosis in neutrophils (Wendler and Tooze, 2001), and early endosome to TGN transport of Shiga toxin (Mallard et al., 2002). Our ability to monitor transport from late endosomes to the TGN in vitro enables us to be precise in specifying one of STX10's functional assignments.

The route of MPR recycling to the TGN

Understanding the routes by which MPRs return to the Golgi complex has been somewhat confused by the observation that depletion of the clathrin adaptor AP-1 (Meyer et al., 2000) and the retromer coat complex (Arighi et al., 2004; Seaman, 2004) leads to the morphological accumulation of MPRs in early endosomes. Because MPRs were seen to accumulate in early endosomes in AP-1–depleted cells and because retromer subunits themselves localize to early endocytic compartments, some have concluded that transport to the Golgi might occur directly from early endosomes.

There is no question that AP1 and retromer are essential for MPR transport. However, the additional requirement for the late endosomal Rab9 GTPase (Lombardi et al., 1993; Riederer et al., 1994; Iversen et al., 2001; Ganley et al., 2004) must be incorporated into any model for MPR recycling. Expression of endogenous levels of a dominant-negative Rab9 mutant triggers the missorting of lysosomal enzymes, inhibits the return of CI-MPRs to the TGN (as monitored directly by their failure to be resialylated), increases the cell surface pool of MPRs, and induces the compensatory expression of MPRs and other lysosomal enzymes (Riederer et al., 1994). Loss of Rab9 by siRNA has similar phenotypic consequences (Ganley et al., 2004), and the addition of Rab9 stabilizes MPRs in cells in which Rab9 function is compromised (Ganley and Pfeffer, 2006). The same is true in cells lacking the Rab9 effectors TIP47 (Diaz and Pfeffer, 1998; Ganley et al., 2004) and GCC185 (Reddy et al., 2006): the loss of either of these effectors strongly destabilizes MPRs. Thus, although a direct path from early endosomes to the Golgi might be viewed as the simplest model, many lines of evidence show that cells use the late endosomal Rab9 and its effectors for biochemically scored MPR return to the Golgi.

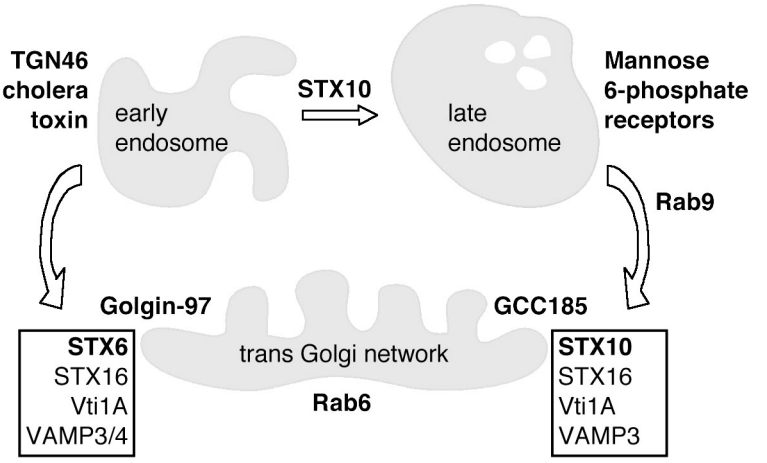

Figure 9. **Summary diagram showing the distinct molecular requirements for transport from late endosomes and early endosomes to the TGN.** See Discussion for details. A role for STX6 in cholera toxin transport is shown here. A role for STX6, Vti1a, and STX16 in Shiga toxin transport was shown by Mallard et al. (2002), and a role for STX16 was shown by Wang et al. (2005). STX16 has also been shown to participate in cholera toxin recycling (Amessou et al., 2007). Therefore, we assume that cholera and Shiga toxins are using the same STX6 complex.

At steady state, MPRs are localized predominantly in perinuclear late endosomes, as determined by quantitative electron microscopy in conjunction with specific antibody labeling procedures (Griffiths et al., 1988). Without double labeling for Golgi markers, perinuclear, late endosomal MPRs cannot be distinguished from the closely apposed (and even intertwined) Golgi complex (Barbero et al., 2002). Live cell video microscopy has shown that MPRs first leave the Golgi in tubulovesicular carriers and are delivered to early endosomes (Waguri et al., 2003); the receptors then return to the perinuclear region, and, at steady state, most arrive in late endosomes. Live cell video microscopy has also detected the direct transfer of vesicles from Rab9-positive late endosomes to distinctly labeled Golgi complexes marked with GFP-galactosyltransferase (Barbero et al., 2002). Transport of the native MPR from late endosomes to the Golgi is a relatively slow process (Duncan and Kornfeld, 1988) that is not always accurately recapitulated by GFP-tagged MPR proteins (Waguri et al., 2006). MPRs shift from late endosomes to early endosomes when cells are depleted of AP1 or retromer (Arighi et al., 2004; Seaman, 2004). The simplest way to incorporate all of the published data are to propose that AP1 and retromer proteins function before MPRs arrive in late endosomes. Alternatively, some MPRs may traverse back directly from early endosomes, but Rab9, its effectors, and, in human cells, STX10 must still somehow participate.

Importantly, the molecular distinction between STX10- and Rab9-independent early endosome to Golgi transport of TGN46 and Shiga and cholera toxin versus the STX10/Rab9-dependent transport of MPRs documented here provides molecular proof of the distinction between these two transport routes (Fig. 9). The t-SNARE that receives cargo from early endosomes, STX6, is dispensible for MPR recycling in these cells. In summary, there is no question that retromer is important for MPR export from early endosomes, together with Shiga toxin export from the same compartment (Bujny et al., 2007; Popoff et al., 2007). However, these cargoes clearly diverge after a retromer-dependent step, as seen by their subsequent differential requirements for STX10 shown here.

Our finding that GCC185 can bind to STX16 raises several interesting questions. The STX16 t-SNARE is part of more than one SNARE complex, but GCC185 seems to be most important for the STX10-dependent receipt of cargoes arriving at the Golgi from late endosomes. It is important to acknowledge that our SNARE binding studies analyzed the association of soluble, nonnative SNARE proteins with their endogenous partners. Although the binding was highly specific, it is not clear that the soluble SNARE proteins will engage only catalytically competent SNARE complexes. We still do not fully understand how SNAREs themselves are localized and how functional, trimeric t-SNARE complexes relate in equilibrium with other SNARE complex subassemblies within biological membranes. Further analysis of the STX10- and STX6-containing SNARE complexes will resolve some of these questions. We are most excited about the prospect that tethers such as GCC185 may contribute to SNARE complex assembly, which was shown most elegantly for p115 in Golgi–SNARE complex assembly (Shorter et al., 2002).

Rab6 is localized to the Golgi complex and may participate in recruiting cytosolic GCC185 to that compartment. We have shown here that Rab6 can compete with STX16 for interaction with GCC185 and that binding involves common amino acid residues near GCC185's C terminus. This suggests that Rab6 can regulate the binding of STX16 to GCC185. If tethers interact with SNARE proteins to catalyze SNARE complex assembly, it is also important for tethers to be removed from such complexes so that they can drive membrane fusion. An appealing possibility is that Rab6 modulates a tether-mediated SNARE assembly reaction. Alternatively, Rab GTPases template the formation of functional membrane microdomains (Pfeffer, 2001; Zerial and McBride, 2001). Perhaps Rab–tether and tether–SNARE interactions recruit these proteins to a given membrane microdomain and, thereby, facilitate their ability to function. The functional consequences of Rab–tether and tether–SNARE interactions will be important areas for future investigation.

Materials and methods

Expression plasmids, recombinant proteins, and antibodies

SNARE protein DNA sequences lacking a transmembrane domain were amplified from full-length cDNA clones obtained from American Type Culture Collection or Deutsches Ressourcenzentrum für Genomforschung (RZPD) and verified by sequencing. DNA sequences were cloned into the

GST fusion vector pGEX4T-1 (GE Healthcare) or pGEX6P-1 for Vti1b and transformed in *Escherichia coli* BL21(DE3) cells. Cytosolic, soluble domains of STX6 (mammalian gene collection 12919; residues 1–230; American Type Culture Collection), STX12 (IRATp970G0973D; residues 1–245; RZPD), VAMP3 (mammalian gene collection 14563; residues 1–75; American Type Culture Collection), VAMP4 (residues 1–110; a gift from R.H. Scheller, Genentech, South San Fransisco, CA), VAMP7 (IRATp970D0710D; residues 1–182; RZPD), and VAMP8 (mammalian gene collection 1585; residues 1–70; American Type Culture Collection) were induced with 0.5 mM IPTG for 2 h at 37°C. STX11 (IRATp970B0847D; residues 1–277; RZPD), STX16 (mammalian gene collection 90328; residues 1–296; American Type Culture Collection), Vti1a (mammalian gene collection 9292; residues 1–192; American Type Culture Collection), and Vti1b (mammalian gene collection 3767; residues 1–202; American Type Culture Collection) were induced with 0.5 mM IPTG for 4 h at 30°C. STX10 (mammalian gene collection 19625; residues 1–222; American Type Culture Collection was induced with 0.5 mM IPTG at room temperature for 6 h. Cells were resuspended to 40 ml in cytosol buffer (25 mM Hepes, pH 7.4, 50 mM KCl, 1 mM $MgCl_2$, and 0.5 mM EDTA) containing 1 mM PMSF, 1 mM DTT, and DNase I. Cells were lysed using a French press, and lysates were centrifuged at 20,000 rpm for 30 min in a JA 20 rotor (Beckman Coulter). GST-SNAREs were purified from clarified lysates using glutathione 4B–Sepharose beads (GE Healthcare) and eluted with cytosol buffer containing 20 mM glutathione, pH 7.4, which was then removed by dialysis.

GST-STX10 was also purified and refolded from inclusion bodies. Bacterial pellets were resuspended in 50 mM Tris, pH 8.0, 25% sucrose (wt/vol), 10 mM DTT, and 1 mM PMSF, lysed by French press, and clarified by a 30-min spin at 20,000 rpm in a JA-20 rotor. Pellets were resuspended three times and centrifuged at 10,000 rpm for 10 min in isolation buffer (20 mM Tris, pH 8.0, 2 M urea, 0.5 M NaCl, and 2% Triton X-100) and dissolved in solubilization buffer (20 mM Tris, 6 M guanidine HCl, 0.5 mM NaCl, 4 mM DTT, and 1 mM 2-mercaptoethanol, pH 8.0) for 1 h at room temperature with gentle agitation. Samples were flash frozen and stored at −80°C. For refolding, 2 ml of solubilized inclusion bodies was added dropwise from a 25-gauge needle to 200 ml of refolding buffer (100 mM Tris, pH 8.0, 400 mM L-arginine, 2 mM EDTA, 5 mM of reduced glutathione, 0.5 mM oxidized glutathione, and 1 mM PMSF) at 4°C with constant stirring. After 15 h and an additional 8 h, another 2 ml of inclusion bodies was added. 15 h after the last addition, the sample was centrifuged at 40,000 rpm in a 45 Ti rotor (Beckman Coulter). The supernatant was concentrated and desalted into cytosol buffer using PD-10 columns (GE Healthcare). Correctly folded protein was isolated using glutathione 4B–Sepharose beads as before.

The GST-tagged C-terminal 110–amino acid fragment of GCC185 (C-110) was purified as described previously (Reddy et al., 2006). For binding assays, the GST tag of C-110 was removed during purification using 20 U/ml thrombin (Sigma-Aldrich) for 2 h at room temperature. Thrombin was neutralized by the addition of 10 mM benzamidine (Sigma-Aldrich) followed by dialysis into 50 mM Hepes, pH 7.6, and 250 mM KCl. His-tagged (6×) human Rab6A in pET15b (a gift from T. Meyer, Stanford, Stanford, CA) was transformed into *E. coli* BL21(DE3) cells for protein expression. Cells (0.8 OD_{600}) were induced for 16 h at room temperature with 0.5 mM IPTG. Cells were resuspended to 40 ml in lysis buffer (50 mM Tris, pH 8.0, 200 mM NaCl, 10 mM imidazole, 5 mM $MgCl_2$, 0.2 mM DTT, and 10 μM GDP) containing 1 mM PMSF. Cells were lysed using a French press, and lysates were centrifuged at 20,000 rpm for 30 min in a JA 20 rotor. His-Rab6A was purified using Ni-NTA agarose (QIAGEN) and eluted with lysis buffer containing 200 mM imidazole followed by dialysis in 50 mM Tris, pH 8.0, 150 mM KCl, 5 mM $MgCl_2$, 1 mM EDTA, and 10 μM GDP. Polyclonal antibodies against STX6, 10, 16, and Vti1a were gifts from J.E. Rothman (Columbia University, New York, NY). Monoclonal antibodies against STX6 were gifts from R.H. Scheller. Mouse anti–Golgin 97 was purchased from Invitrogen, sheep anti-TGN46 was obtained from Serotec, and rabbit anti-STX6 (C-19), which was used for immunofluorescence, was purchased from Santa Cruz Biotechnology, Inc. Rabbit anti–sorting nexin-2 antibodies were gifts from C.R. Haft (National Institutes of Health, Bethesda, MD). Mouse anti-myc, rabbit anti-GST, and rabbit anti-GCC185 have been described previously (Reddy et al., 2006).

Cell culture

HeLa and HEK293 cells were cultured and transfected as described previously (Ganley and Pfeffer, 2006). RNAi was performed using siRNAs from Dharmacon. STX10 mRNA was targeted with the sequences GGAAGAGACCATCGGTATA or TATCCCACATGACGAGTGA, and both siRNAs showed identical phenotypes. GACATCTTTGATCACCAGA was used to target STX6. siRNA directed against STX16 was described previously (Wang et al., 2005). siRNA directed against GFP was used as a negative control (Chi et al., 2003). Specific silencing of targeted genes was confirmed in at least three independent experiments.

Assays

In vitro transport assays were performed as described previously (Reddy et al., 2006). Purified GST or GST-SNAREs were added at 100 μg/ml (unless otherwise stated) before 90 min of in vitro transport at 37°C. Pulse-chase turnover experiments were performed as described previously (Ganley et al., 2004); radioactive precursor was added 38.5 h after siRNA transfection. Labeling was performed for 1.5 h. Samples were analyzed for MPR degradation beginning 48 h after siRNA addition when STX10 depletion was significant.

Hexosaminidase secretion

Assays were performed as described previously (Riederer et al., 1994). HeLa cells were transfected with myc-tagged cytosolic SNARE constructs for 24 h or with STX10/control siRNAs for 72 h. Cells were incubated in phenol red–free DME supplemented with 10 mM mannose 6-phosphate (Sigma-Aldrich) for 8 h before assay. Myc-tagged cytosolic STX6, Vti1a, VAMP3, and VAMP4 contained LEHASRGPYSIVSPKC C terminal to the cytosolic domain.

Immunofluorescence microscopy and immunoblots

Cell fixation, staining, and mounting in mowiol were described previously (Ganley et al., 2004). Goat anti–rabbit AlexaFluor488 and goat anti–mouse AlexaFluor594 were used. Micrographs in Figs. 4 A, 5 (A and B), 6, and S1 were acquired using a microscope (Axioplan2; Carl Zeiss, Inc.) fitted with a 63×/NA 1.30 plan Neofluar objective lens and a CCD camera (AxioCamHRc; Carl Zeiss, Inc.) and controlled by Axiovision 4.6 software (Carl Zeiss, Inc.). Pictures were analyzed using Photoshop (Adobe). Fig. 4 (C and D) was obtained with a deconvolution microscopy system (Spectris; Applied Precision) with an inverted epifluorescence microscope (IX70; Olympus), a plan Apo 60×/1.40 NA oil immersion objective (Olympus), a CCD camera (CoolSNAP HQ; Roper Scientific), and DeltaVision acquisition and deconvolution software (Applied Precision). Some images quantified in 4D were also acquired using a spectral confocal microscope system (DM6000B; Leica) using a 63×/NA 1.40 lens and confocal software (Leica). The perinuclear region (mean area of 54 μm^2) was excluded from the analysis to ensure characterization of nonlate endosome structures. Immunoblot analysis and quantification of proteins were previously described (Ganley et al., 2004).

Cholera toxin uptake

HeLa cells transfected with the indicated siRNAs for 72 h were grown on glass coverslips and incubated in media containing 4 μg/ml cholera toxin B subunit conjugated to AlexaFluor488 (Invitrogen) for 30 min at 37°C followed by washing and a chase of 30 min at 37°C in toxin-free media. Cells were then fixed and stained for immunofluorescence.

Binding assays

1 μM of purified GST–cytosolic SNARE proteins was incubated with 2 μM GCC185 C-110 in a volume of 300 μl of binding buffer (20 mM Hepes, pH 7.6, 250 mM KCl, 5 mM $MgCl_2$, 0.2% Triton X-100, 0.1 mg/ml BSA, and 0.2 mM DTT) for 1 h with rotation at room temperature. GST-SNAREs were recovered using glutathione–Sepharose beads and washed three times in binding buffer. The amount of GCC185 C-110 associating with the GST-SNARE was determined by SDS-PAGE and immunoblotting. For binding assays involving His-Rab6, the Rab was first preloaded with nucleotide for 2 h at room temperature by incubating in 20 mM Hepes, pH 7.6, 150 mM KCl, 2 mM EDTA, 1 mM $MgCl_2$, 0.1 mg/ml BSA, 0.1 mM DTT, and 1 mM GDP or 1 mM GTPγS (Sigma-Aldrich). The concentration of Rab6 in the binding assay was 0.7 μM.

Cytosolic GCC185 binding to GST-SNAREs

0.4 nmol GST–cytosolic SNARE was incubated with 700 μg K562 cytosol (Itin et al., 1997) in 0.5 ml of binding buffer for 1 h at room temperature with rotation. GST-SNAREs were isolated with glutathione–Sepharose beads and washed in binding buffer, and the associated proteins were analyzed by SDS-PAGE and immunoblotting.

Coimmunoprecipitation

HEK293 cells grown in 10-cm plates were transfected with the indicated myc-tagged cytosolic SNARE constructs. After transfection (24 h), cells were placed on ice, washed three times in ice-cold PBS, and lysed in 1 ml of

immunoprecipitation buffer (50 mM Tris, pH 8.0, 50 mM KCl, 5 mM EDTA, and 1% Triton X-100) containing protease inhibitor cocktail (Roche). Samples were centrifuged at maximum speed for 15 min at 4°C in a microfuge (model 5415; Eppendorf) followed by preclearing with protein A–agarose (prewashed in immunoprecipitation buffer; Roche) for 30 min at room temperature with rotation. Samples were then divided in two and incubated with 10 µl rabbit anti-GCC185 or normal rabbit serum containing an equivalent amount of IgG for 1.5 h at room temperature. Immune complexes were isolated by 30-min incubation with protein A–agarose followed by three washes in immunoprecipitation buffer and one wash in PBS. Immunoprecipitated proteins were analyzed by SDS-PAGE and immunoblotting.

Online supplemental material

Fig. S1 shows the results for four different anti-STX6 antibodies that do not inhibit in vitro transport compared with anti-STX16 antibodies that do. Also, we find that endocytosed cholera toxin B returns to the Golgi in cells depleted of GCC185 protein. Online supplemental material is available at http://www.jcb.org/cgi/content/full/jcb.200707136/DC1.

We are grateful to Wanjin Hong for encouraging us to try human cells as a host for our in vitro transport assay because of anti-SNARE antibody specificity, Drs. Jason Meyer and Pat Brown for the HeLa cell cDNA library, and Drs. Richard Scheller, James Rothman, and Carol Renfrew Haft for clones and antibodies.

This work was supported by a grant from the National Institutes of Health to S.R. Pfeffer (NIDDK 37332-21).

Submitted: 20 July 2007
Accepted: 12 December 2007

References

Aivazian, D., R.L. Serrano, and S. Pfeffer. 2006. TIP47 is a key effector for Rab9 localization. *J. Cell Biol.* 173:917–926.

Amessou, M., A. Fradagrada, T. Falguieres, J.M. Lord, D.C. Smith, L.M. Roberts, C. Lamaze, and L. Johannes. 2007. Syntaxin 16 and syntaxin 5 are required for efficient retrograde transport of several exogenous and endogenous cargo proteins. *J. Cell Sci.* 120:1457–1468.

Antonin, W., C. Holroyd, D. Fasshauer, S. Pabst, G.F. Von Mollard, and R. Jahn. 2000a. A SNARE complex mediating fusion of late endosomes defines conserved properties of SNARE structure and function. *EMBO J.* 19:6453–6464.

Antonin, W., C. Holroyd, R. Tikkanen, S. Honing, and R. Jahn. 2000b. The R-SNARE endobrevin/VAMP-8 mediates homotypic fusion of early endosomes and late endosomes. *Mol. Biol. Cell.* 11:3289–3298.

Arighi, C.N., L.M. Hartnell, R.C. Aguilar, C.R. Haft, and J.S. Bonifacino. 2004. Role of the mammalian Retromer in sorting of the cation-independent mannose 6-phosphate receptor. *J. Cell Biol.* 165:123–133.

Barbero, P., L. Bittova, and S.R. Pfeffer. 2002. Visualization of Rab9-mediated vesicle transport from endosomes to the trans-Golgi in living cells. *J. Cell Biol.* 156:511–518.

Bonifacino, J.S., and R. Rojas. 2006. Retrograde transport from endosomes to the trans-Golgi network. *Nat. Rev. Mol. Cell Biol.* 7:568–579.

Brandhorst, D., D. Zwilling, S.O. Rizzoli, U. Lippert, T. Lang, and R. Jahn. 2006. Homotypic fusion of early endosomes: SNAREs do not determine fusion specificity. *Proc. Natl. Acad. Sci. USA.* 103:2701–2706.

Bujny, M.V., V. Popoff, L. Johannes, and P.J. Cullen. 2007. The retromer component sorting nexin-1 is required for efficient retrograde transport of Shiga toxin from early endosome to the trans Golgi network. *J. Cell Sci.* 120:2010–2021.

Carlton, J.G., M.V. Bujny, B.J. Peter, V.M. Oorschot, A. Rutherford, R.S. Arkell, J. Klumperman, H.T. McMahon, and P.J. Cullen. 2005. Sorting nexin-2 is associated with tubular elements of the early endosome, but is not essential for retromer-mediated endosome-to-TGN transport. *J. Cell Sci.* 118:4527–4539.

Carroll, K.S., J. Hanna, I. Simon, J. Krise, P. Barbero, and S.R. Pfeffer. 2001. Role of Rab9 GTPase in facilitating receptor recruitment by TIP47. *Science.* 292:1373–1376.

Chi, J.T., H.Y. Chang, N.N. Wang, D.S. Chang, N. Dunphy, and P.O. Brown. 2003. Genomewide view of gene silencing by small interfering RNAs. *Proc. Natl. Acad. Sci. USA.* 100:6343–6346.

Coughlin, S.R. 2005. Protease-activated receptors in hemostasis, thrombosis and vascular biology. *J. Thromb. Haemost.* 3:1800–1814.

Derby, M.C., Z.Z. Lieu, D. Brown, J.L. Stow, B. Goud, and P.A. Gleeson. 2007. The TGN Golgin, GCC185, is required for endosome-to-Golgi transport and maintenance of Golgi structure. *Traffic.* 8:758–773.

Diaz, E., and S.R. Pfeffer. 1998. TIP47: a cargo selection device for mannose 6-phosphate receptor trafficking. *Cell.* 93:433–443.

Diaz, E., F. Schimmoller, and S.R. Pfeffer. 1997. A novel Rab9 effector required for endosome-to-TGN transport. *J. Cell Biol.* 138:283–290.

Duncan, J.R., and S. Kornfeld. 1988. Intracellular movement of two mannose 6-phosphate receptors: return to the Golgi apparatus. *J. Cell Biol.* 106:617–628.

Ganley, I.G., and S.R. Pfeffer. 2006. Cholesterol accumulation sequesters Rab9 and disrupts late endosome function in NPC1-deficient cells. *J. Biol. Chem.* 281:17890–17899.

Ganley, I.G., K. Carroll, L. Bittova, and S. Pfeffer. 2004. Rab9 GTPase regulates late endosome size and requires effector interaction for its stability. *Mol. Biol. Cell.* 15:5420–5430.

Ghosh, P., N.M. Dahms, and S. Kornfeld. 2003. Mannose 6-phosphate receptors: new twists in the tale. *Nat. Rev. Mol. Cell Biol.* 4:202–212.

Goda, Y., and S.R. Pfeffer. 1988. Selective recycling of the mannose 6-phosphate/IGF-II receptor to the trans Golgi network in vitro. *Cell.* 55:309–320.

Griffiths, G., B. Hoflack, K. Simons, I. Mellman, and S. Kornfeld. 1988. The mannose 6-phosphate receptor and the biogenesis of lysosomes. *Cell.* 52:329–341.

Hubbard, T.J., B.L. Aken, K. Beal, B. Ballester, M. Caccamo, Y. Chen, L. Clarke, G. Coates, F. Cunningham, T. Cutts, et al. 2007. Ensembl 2007. *Nucleic Acids Res.* 35:D610–D617.

Huminiecki, L., A.T. Lloyd, and K.H. Wolfe. 2003. Congruence of tissue expression profiles from Gene Expression Atlas, SAGEmap and TissueInfo databases. *BMC Genomics.* 4:31.

Itin, C., C. Rancano, Y. Nakajima, and S.R. Pfeffer. 1997. A novel assay reveals a role for soluble N-ethylmaleimide-sensitive fusion attachment protein in mannose 6-phosphate receptor transport from endosomes to the trans Golgi network. *J. Biol. Chem.* 272:27737–27744.

Iversen, T.G., G. Skretting, A. Llorente, P. Nicoziani, B. van Deurs, and K. Sandvig. 2001. Endosome to Golgi transport of ricin is independent of clathrin and of the Rab9- and Rab11-GTPases. *Mol. Biol. Cell.* 12:2099–2107.

Jahn, R., and R.H. Scheller. 2006. SNAREs–engines for membrane fusion. *Nat. Rev. Mol. Cell Biol.* 7:631–643.

Lin, S.X., W.G. Mallet, A.Y. Huang, and F.R. Maxfield. 2004. Endocytosed cation-independent mannose 6-phosphate receptor traffics via the endocytic recycling compartment en route to the trans-Golgi network and a subpopulation of late endosomes. *Mol. Biol. Cell.* 15:721–733.

Lombardi, D., T. Soldati, M.A. Riederer, Y. Goda, M. Zerial, and S.R. Pfeffer. 1993. Rab9 functions in transport between late endosomes and the trans Golgi network. *EMBO J.* 12:677–682.

Lu, L., G. Tai, and W. Hong. 2004. Autoantigen Golgin-97, an effector of Arl1 GTPase, participates in traffic from the endosome to the trans-golgi network. *Mol. Biol. Cell.* 15:4426–4443.

Luke, M.R., L. Kjer-Nielsen, D.L. Brown, J.L. Stow, and P.A. Gleeson. 2003. GRIP domain-mediated targeting of two new coiled-coil proteins, GCC88 and GCC185, to subcompartments of the trans-Golgi network. *J. Biol. Chem.* 278:4216–4226.

Lupashin, V., and E. Sztul. 2005. Golgi tethering factors. *Biochim. Biophys. Acta.* 1744:325–339.

Mallard, F., B.L. Tang, T. Galli, D. Tenza, A. Saint-Pol, X. Yue, C. Antony, W. Hong, B. Goud, and L. Johannes. 2002. Early/recycling endosomes-to-TGN transport involves two SNARE complexes and a Rab6 isoform. *J. Cell Biol.* 156:653–664.

McBride, H.M., V. Rybin, C. Murphy, A. Giner, R. Teasdale, and M. Zerial. 1999. Oligomeric complexes link Rab5 effectors with NSF and drive membrane fusion via interactions between EEA1 and syntaxin 13. *Cell.* 98:377–386.

Meyer, C., D. Zizioli, S. Lausmann, E.L. Eskelinen, J. Hamann, P. Saftig, K. von Figura, and P. Schu. 2000. mu1A-adaptin-deficient mice: lethality, loss of AP-1 binding and rerouting of mannose 6-phosphate receptors. *EMBO J.* 19:2193–2203.

Mills, I.G., S. Urbe, and M.J. Clague. 2001. Relationships between EEA1 binding partners and their role in endosome fusion. *J. Cell Sci.* 114:1959–1965.

Parham, P. 2005. MHC class I molecules and KIRs in human history, health and survival. *Nat. Rev. Immunol.* 5:201–214.

Pfeffer, S.R. 2001. Rab GTPases: specifying and deciphering organelle identity and function. *Trends Cell Biol.* 11:487–491.

Popoff, V., G.A. Mardones, D. Tenza, R. Rojas, C. Lamaze, J.S. Bonifacino, G. Raposo, and L. Johannes. 2007. The retromer complex and clathrin define an early endosomal retrograde exit site. *J. Cell Sci.* 120:2022–2031.

Prekeris, R., J. Klumperman, Y.A. Chen, and R.H. Scheller. 1998. Syntaxin 13 mediates cycling of plasma membrane proteins via tubulovesicular recycling endosomes. *J. Cell Biol.* 143:957–971.

Pryor, P.R., B.M. Mullock, N.A. Bright, M.R. Lindsay, S.R. Gray, S.C. Richardson, A. Stewart, D.E. James, R.C. Piper, and J.P. Luzio. 2004. Combinatorial SNARE complexes with VAMP7 or VAMP8 define different late endocytic fusion events. *EMBO Rep.* 5:590–595.

Reddy, J.V., A.S. Burguete, K. Sridevi, I.G. Ganley, R.M. Nottingham, and S.R. Pfeffer. 2006. A functional role for the GCC185 golgin in mannose 6-phosphate receptor recycling. *Mol. Biol. Cell.* 17:4353–4363.

Riederer, M.A., T. Soldati, A.D. Shapiro, J. Lin, and S.R. Pfeffer. 1994. Lysosome biogenesis requires Rab9 function and receptor recycling from endosomes to the trans-Golgi network. *J. Cell Biol.* 125:573–582.

Rojas, R., S. Kametaka, C.R. Haft, and J.S. Bonifacino. 2007. Interchangeable but essential functions of SNX1 and SNX2 in the association of retromer with endosomes and the trafficking of mannose 6-phosphate receptors. *Mol. Cell. Biol.* 27:1112–1124.

Rutherford, A.C., C. Traer, T. Wassmer, K. Pattni, M.V. Bujny, J.G. Carlton, H. Stenmark, and P.J. Cullen. 2006. The mammalian phosphatidylinositol 3-phosphate 5-kinase (PIKfyve) regulates endosome-to-TGN retrograde transport. *J. Cell Sci.* 119:3944–3957.

Saint-Pol, A., B. Yelamos, M. Amessou, I.G. Mills, M. Dugast, D. Tenza, P. Schu, C. Antony, H.T. McMahon, C. Lamaze, and L. Johannes. 2004. Clathrin adaptor epsinR is required for retrograde sorting on early endosomal membranes. *Dev. Cell.* 6:525–538.

Schweizer Burguete, A., T.D. Fenn, A.T. Brunger, and S.R. Pfeffer. 2008. Rab and Arl GTPase family members cooperate in the localization of the Golgin GCC185. *Cell.* In press.

Seaman, M.N. 2004. Cargo-selective endosomal sorting for retrieval to the Golgi requires retromer. *J. Cell Biol.* 165:111–122.

Shorter, J., M.B. Beard, J. Seemann, A.B. Dirac-Svejstrup, and G. Warren. 2002. Sequential tethering of Golgins and catalysis of SNAREpin assembly by the vesicle-tethering protein p115. *J. Cell Biol.* 157:45–62.

Skrabanek, L., and F. Campagne. 2001. TissueInfo: high-throughput identification of tissue expression profiles and specificity. *Nucleic Acids Res.* 29:e102.

Smith, D.C., R.A. Spooner, P.D. Watson, J.L. Murray, T.W. Hodge, M. Amessou, L. Johannes, J.M. Lord, and L.M. Roberts. 2006. Internalized Pseudomonas exotoxin A can exploit multiple pathways to reach the endoplasmic reticulum. *Traffic.* 7:379–393.

Spooner, R.A., D.C. Smith, A.J. Easton, L.M. Roberts, and J.M. Lord. 2006. Retrograde transport pathways utilised by viruses and protein toxins. *Virol. J.* 3:26.

Sun, W., Q. Yan, T.A. Vida, and A.J. Bean. 2003. Hrs regulates early endosome fusion by inhibiting formation of an endosomal SNARE complex. *J. Cell Biol.* 162:125–137.

Tai, G., L. Lu, T.L. Wang, B.L. Tang, B. Goud, L. Johannes, and W. Hong. 2004. Participation of the syntaxin 5/Ykt6/GS28/GS15 SNARE complex in transport from the early/recycling endosome to the trans-Golgi network. *Mol. Biol. Cell.* 15:4011–4022.

Tong, P.Y., and S. Kornfeld. 1989. Ligand interactions of the cation-dependent Mannose 6-phosphate receptor. Comparison with the cation-independent Mannose 6-phosphate receptor. *J. Biol. Chem.* 264:7970–7975.

Waguri, S., F. Dewitte, R. Le Borgne, Y. Rouille, Y. Uchiyama, J.F. Dubremetz, and B. Hoflack. 2003. Visualization of TGN to endosome trafficking through fluorescently labeled MPR and AP-1 in living cells. *Mol. Biol. Cell.* 14:142–155.

Waguri, S., Y. Tomiyama, H. Ikeda, T. Hida, N. Sakai, M. Taniike, S. Ebisu, and Y. Uchiyama. 2006. The luminal domain participates in the endosomal trafficking of the cation-independent mannose 6-phosphate receptor. *Exp. Cell Res.* 312:4090–4107.

Wakeham, D.E., L. Abi-Rached, M.C. Towler, J.D. Wilbur, P. Parham, and F.M. Brodsky. 2005. Clathrin heavy and light chain isoforms originated by independent mechanisms of gene duplication during chordate evolution. *Proc. Natl. Acad. Sci. USA.* 102:7209–7214.

Wang, Y., G. Tai, L. Lu, L. Johannes, W. Hong, and B. Luen Tang. 2005. Trans-Golgi network syntaxin 10 functions distinctly from syntaxins 6 and 16. *Mol. Membr. Biol.* 22:313–325.

Wendler, F., and S. Tooze. 2001. Syntaxin 6: the promiscuous behaviour of a SNARE protein. *Traffic.* 2:606–611.

Zerial, M., and H. McBride. 2001. Rab proteins as membrane organizers. *Nat. Rev. Mol. Cell Biol.* 2:107–117.